Design of a Compact MIMO Antenna for Bluetooth and Wi-Fi Applications

Dr.P.P.Priya[1], B.Sirisha[2], D.Gowri[3], S.Mounavi[4], B.Sravani[5]
[1]putchapoornapriya@gmail.com
[2]sirishabarnikana2@gmail.com
[3]gowridasu09@gmail.com
[4]simhadri.mounavi1@gmail.com
[5]sravanibera123@gmail.com

***Abstract*: The proposed MIMO antenna consists of two single antennas, each having size of 13*12.8 mm^2, symmetrically arranged next to each other. The single and MIMO antennas are simulated and analyzed. To verify the simulated results, The prototype antennas were fabricated and measured. A good agreement between measurements and simulations is obtained. The proposed antenna covers the 2.4GHz band (2-5 GHz) allocated by the FCC. The MIMO parameters, such as diversity gain (DG), total active reflection coefficient (TARC), realized gain, and efficiency, are efficiency, are also studied. Thus, the results demonstrate that our antenna is suitable for Bluetooth and WIFI Applications.**

Keywords: **FCC, MIMO**.

I. INTRODUCTION

In any wireless communication field antenna is a primary need. There are many antennas are available based on the specified requirements. Both WIFI antennas and Bluetooth antennas are operated between the range of 2.4GHz to 2.5GHz frequency band. The range of WIFI antennas reaches a few kilometers, whereas the Bluetooth antennas operates at a range of 100m away. As the antenna depends on frequency, not on content. Microstrip patch antenna is best suitable for these Bluetooth and WIFI applications, as it operates at satellite communication which resonates at 2.4GHz frequency.

II. LITERATURE SURVEY

As the same antenna is going to be used in the two different applications, then first we need to understand the concepts of

- Bluetooth (IEEE 802.15)
- WIFI (IEEE 802.11)
- Microstrip patch antenna
- MIMO

The Bluetooth and WIFI are the electronic devices, which provide the communication between two devices without having any cables. Physically, the application is same, but the ranges are different. Microstrip patch is also known as printed antenna covers the overall frequency range of Bluetooth and WIFI.

The main concern of doing this type of antenna is to make the size compact, to increase the Bandwidth in order to carry large data and moreover, as the same antenna for both different applications. So, it is easy to use as per our requirement.

MIMO (multiple input multiple output) is an antenna technology for wireless communications in which multiple antennas are used at both the source and destination. The main use is to minimize the errors, improve data rates, and creates multiple paths for communication.

III. MATHEMATICAL SUPPORT FOR PROPOSED ANTENNA

Two antenna models are investigated and proposed in this work. The antenna model 1 and antenna model 2, exhibits broadband characteristics and dual band characteristics respectively.

For calculating the characteristic impedance

$$Z_{\text{om}} = \frac{\eta}{2\pi\sqrt{\epsilon_{re}}} \ln\left(\frac{8h}{W} + 0.25\frac{W}{h}\right) \quad for\ (\frac{W}{h} \geq 1) \quad \text{-----(1)}$$

Where ε_{re}=Effective Dielectric Constant

When the characteristic impedance of the microstrip line is known then to find the width of the strip is given by

$$\frac{W}{h} = \frac{2}{\pi}\{\frac{60\pi^2}{Z_{om}\sqrt{\epsilon_r}} - e1 - \ln\left(\frac{120\pi^2}{Z_{om}\sqrt{\epsilon_r}} - 1\right) + \frac{\epsilon_r - 1}{2\epsilon_r}[\ln(\frac{60\pi^2}{Z_{om}\sqrt{\epsilon_r}} - 1) + 0.39 - \frac{0.61}{\epsilon_r}]\} \text{ ---(2)}$$

For an efficient radiator, the optimized width is given as

$$W = \frac{1}{2f_r\sqrt{\epsilon_0\mu_0}}\sqrt{\frac{2}{\epsilon_r + 1}} \quad \text{--- (3)}$$

Where, ϵ_0=Permitivity Constant

μ_0=Permeability Constant

The length of the patch can be determined by

$$L = \frac{1}{2f_r\sqrt{\epsilon_{re}}\sqrt{\epsilon_0\mu_0}} - 2\Delta L \quad \text{----(4)}$$

The normal modes refer to the source free fields which can exist in the region between the patch and ground plane. This region is modelled as a cavity bounded by electric walls in the top and bottom and magnetic walls on the side., under the assumptions that the thickness is much less than the wavelength, the electric field has only the vertical component E_z which is independent of z and satisfies the homogenous equation.

$$(\nabla^2 + k_d^2)E_z = 0 \quad \text{---(5)}$$

And the boundary condition $\overline{h_t} = 0$ on the side walls of the cavity. In the cylindrical coordinates, eq.(5) reads

$$\frac{1}{\rho}\frac{\partial}{\partial\rho}\left(\rho\frac{\partial E_z}{\partial p}\right) + \frac{1}{\rho^2}\frac{\partial^2 E_z}{\partial\varphi^2} + \frac{\partial^2 E_z}{\partial z^2} = -k_d^2 E_z \text{-(6)}$$

Due to the assumption of the cavity model,

$$\frac{\partial^2 E_z}{\partial z^2} = 0$$

Using the method of the separation of variables, we let

$$E_z = P(\rho)Q(\varphi) \quad \text{---- (7)}$$

Equation (6) becomes

$$\frac{\rho}{\rho}\frac{\partial}{\partial\rho}\left(\rho\frac{\partial p}{\partial p}\right) + k_d^2\rho^2 = -\frac{1}{Q}\frac{\partial^2 Q}{\partial\varphi^2} \quad \text{------ (8)}$$

Since the right-hand side depends on and the left-hand side depends on $\sin n\varphi$ only, we have the following equations for the functions Q and P.

$$\frac{1}{Q}\frac{\partial^2 Q}{\partial\varphi^2} = -n^2 \quad \text{------ (9)}$$

$$\rho^2\frac{\partial^2 Q}{\partial\varphi^2} + \rho\frac{\partial p}{\partial\rho} + [(k_d\rho)^2 - n^2]P = 0$$

------ (10)

The solution for Q is

$$Q = C_1 \quad \text{------- (11)}$$

Where n is an integer since Q must be periodic with period 2π.

The solution for P is

$$P = c_{2J_n(k_d\rho)+c_3Y_n(k_d)\rho} \quad \text{------- (12)}$$

Where J_n is the Bessel function of the first king of order n and Y_n is the Bessel function of the second kind of order n.

Since fields are infinite at ρ=0,$e_3 = 0$.

Thus

$$E_z = E_0 J_n(k_d\rho)\cos n\varphi \quad \text{----- (13)}$$

From maxwell's equations, we obtain

$$H_\rho = -j\frac{\omega\varepsilon n}{k^2\rho}E_0 J_n(k_d\rho)\sin n\varphi \quad \text{---- (14)}$$

$$H_\varphi = -j\frac{\omega\varepsilon n}{k}E_0 J'_n(k_d\rho)\cos n\varphi \quad \text{--- (15)}$$

Where $J'_n(k_d\rho)$ is the derivative of $J_n(k_d\rho)$ with respect to the argument $(k_d\rho)$.Applying magnetic wall boundary condition, we have

$H_\varphi = 0|_{\rho=a} \rightarrow J'_n(k_d a)=0$ --- (16)

Let the roots of (11) be X_{nm}. Then the eigen values of k_d, denoted by $K_{nm,}$ are:

$$K_{nm} = \frac{X_{nm}}{a} \quad \text{-------- (17)}$$

The resonant frequency of a TM_{nm} mode is

$$f_{nm} = \frac{X_{nm}}{2\pi a\sqrt{\mu_0 \varepsilon}} = \frac{X_{nm}c}{2\pi a\sqrt{\varepsilon_r}} \quad \text{--- (18)}$$

$$a_e = a[1 + \frac{2t}{\pi a \varepsilon_r}\ln(\frac{\pi a}{2t} + 1.7726)]^{1/2} \text{--- (19)}$$

Using a_e, the resonant frequency formula becomes

$$f_{nm} = \frac{X_{nm}c}{2\pi a\sqrt{\varepsilon_r}} \quad \text{---- (20)}$$

Circularly polarized waves can be provided by diagonal-fed patch with a pair of notches or stubs along with two opposite edges. The slot edges and feeding position are modified by considering orthogonal modes of same magnitude and phase difference. To attain impedance bandwidth with good circular polarization Two-fold stubs are placed in the design. A commercial FR4 substrate with dielectric constant ε_r=4.4 and dielectric loss tangent i.e., tan =0.02 is used in the proposed design of antennas. The rotation of square slot away from the feedline is done in this design. The total perturbation area A is obtained by

$$\left(\frac{\Delta A}{A}\right) Q_0 \cong \frac{1}{2} \quad \text{---- (21)}$$

Where, A is area of square patch without perturbations and Q_0 is quality factor of patch. Slot antenna is designed determinately by selecting the stub length. To obtain impedance matching and good circular polarization performance from the antenna, slot stub length is designed and varied. The designed characteristics antenna structures are shown in the below figure-1.

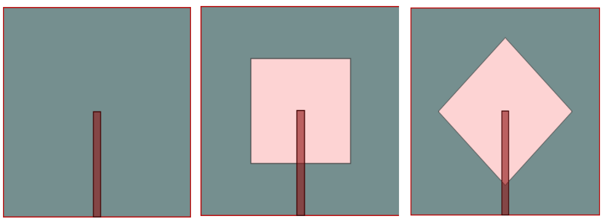

(a) (b) (c)

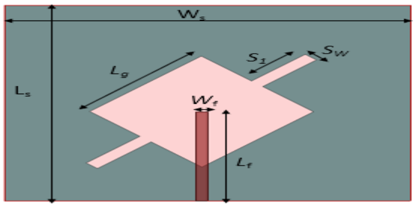

(d)

Fig 1. Iterations of the proposed Antenna model

The parametric definitions and optimized dimensions of Wideband antenna with defected ground structure is illustrated in table-1.

Table 1. Parametric Definitions of single Feed Antenna

Parameter	Definition	Value in mm
L_s	Length of Antenna	80
W_s	Width of Antenna	80
L_f	Length of Feed	40
W_f	Width of Feed	3.2
L_g	Length of Ground slot	40
S_l	Length of stub	15.5
S_w	Width of stub	4

IV. RESULTS AND ANALYSIS

The proposed antenna models are designed and simulated through HFSS and the results are presented in this section.

4.1 Return Loss Vs Frequency Characteristics

Figure-2 gives the reflection characteristics of the antenna. The basic antenna model doesn't operate at any frequency in antenna 2 operates at the resonance frequency of 2 GHz with S11 of -12dB with bandwidth of 0.3GHz. The antenna 3 operates at resonance frequency of 2.1 GHz with S11 of -25dB with bandwidth of 0.36 GHz. The proposed antenna 4 operates at dual frequency band at resonating frequencies of 1.85 GHz and 2.77 GHz and covering frequency range of 1.6-2.32 GHz and second frequency band of 2.5-2.99 GHz. The dual band antenna notching the frequency band of

2.3-2.6 GHz, where Wireless LAN and Bluetooth applications are blocked which are used by many wireless communication units.

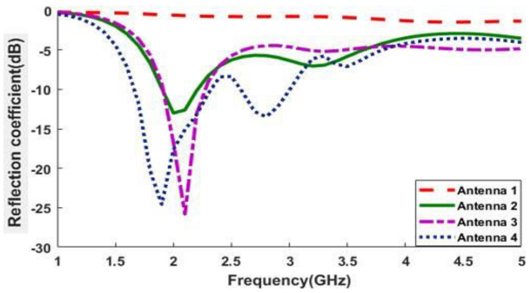

Fig 2. Reflection Coefficient of Antenna

Iterations % for the antenna 2 and whereas antenna 3 is showing impedance bandwidth of and 17% at resonant band. The impedance bandwidth is 36% and 17% is observed at the proposed antenna which is operating in dual frequency bands.

4.2 Impedance Characteristics

Figure represents the impedance characteristics of the antenna iterations. For the antenna 2 with impedance line touches the 50Ω impedance lines at the operating frequency of 1.9-2.2. Similarly, antenna 3 touches the 50Ω impedance lines of operating frequencies. The antenna 4 operates in frequency of 1.6-2.32 GHz and 2.5-2.99 GHz at these frequencies impedance line touches very near to 50Ω line.

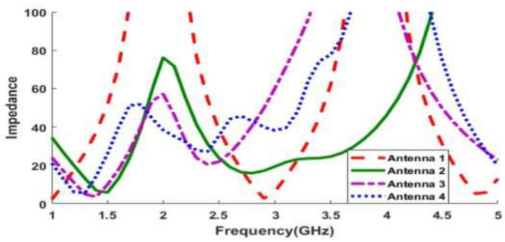

Fig.3. Impedance Characteristics of Antenna Iterations

4.3 Surface Current Distribution Characteristics

The surface current distribution of the antenna models is presented in Fig 4 in the antenna 1 model the current is distributed only along the feed line. For antenna 3 most of the current density is compacted around the feed line whereas for antenna mode compacted current density is observed more at lower half patch and slotted ground structure. The radiating element is contributing radiation rather than slotted ground.

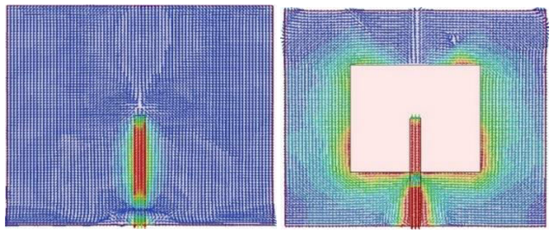

(a) (b)

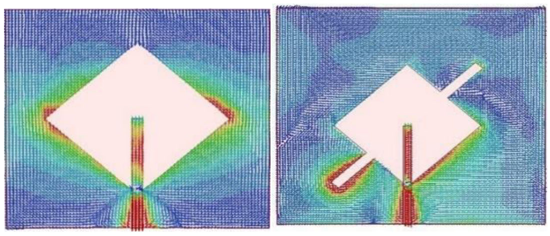

(c) (d)

Fig 4. Surface Current Distribution of Antenna Iterations

4.4 Peak Gain Characteristics

The peak gain of antenna shown in Fig 5. For the antenna 1 shows the negative gain which is not preferable. With the modification of the structure 2, antenna is modified. The variation of gain is changed to positive and provides the maximum gain of 2dBi at the resonating frequency. For the antenna 2 and antenna 4 maximum gain of 4.78dBi is perceived at the resonating frequencies.

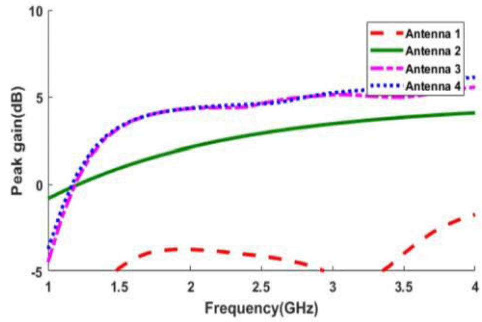

Fig 5. Peak Gain of Antenna Iterations

4.5 Radiation Patterns at Different Frequencies:

The designed antenna radiation characteristics are presented in fig 6. The radiation pattern is dipole like radiation at 1.85 GHz provided by the antenna in the desired direction. The dual band antenna radiation characteristics are presented. The maximum gain is 4.83dB at 1.85 GHz and 4.9dB at 2.77 GHz. Monopole like radiation is at all the resonating frequencies are maintained by antenna models and also observed very low gain at notch band.

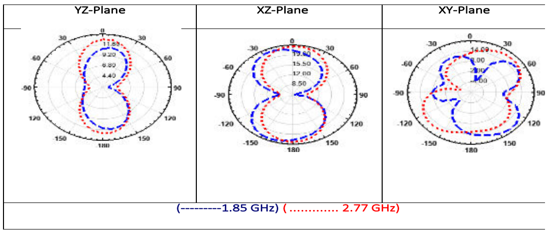

Fig 6. Radiation patterns of antenna 4 at the resonating Frequencies of 1.85 GHz and 2.77 GHz

V. Conclusion

In this paper, a two-port, multiple-input, multiple-output antenna with high isolation and low correlation for Bluetooth and WIFI applications was presented. This antenna is a symmetrical arrangement of two single antennas having a compact size of 12.8x13x1.6 mm^3. Prototype antennas are manufactured and measured. A good agreement is obtained between measurements and simulations. The measured bandwidths of the proposed antennas cover the 2.4 GHz band (2-5 GHz) allocated by the Federal Communications Commission for Bluetooth and WIFI applications. The isolation between the two elements of the MIMO antenna is 41.36 dB at the resonant frequency. Using the spatial diversity technique, high isolation was achieved without adding any other technique. The envelope correlation coefficient has a value of 1.15 10− 7, whereas the diversity gain is around 10 dB, while the TARC is less than − 10 dB in the operating band. Moreover, the gain and efficiency of the proposed MIMO antenna are also analysed and are shown to be satisfactory. The results show that the proposed antenna has the main advantages, such as compact size, high isolation, and low ECC when compared to other works. As a consequence, the proposed antenna may be useful for Bluetooth and WIFI applications.

REFERENCES

[1] B. Fady, J. Terhzaz, A. Tribak, F. Riouch, and A. Mediavilla Sanchez, "Novel miniaturized planar low-cost multiband antenna for industry 4.0 communications," Progress In Electromagnetics Research C, vol. 93, pp. 29–38, 2019.

[2] "5G. Vision.", . https://5g-ppp.eu/wp-content/uploads/2015/ 02/5G-Vision-Brochure-v1.pdf, 2020.

[3] "Les enjeux de la 5g," 2017, https://www.arcep.fr/uploads/tx_ gspublication/rapport-enjeux-5G_mars2017.pdf, 2020.

[4] T. S. Rappaport, Y. Xing, G. R. MacCartney, A. F. Molisch, E. Mellios, and J. Zhang, "Overview of millimeter wave communications for fifth-generation (5G) wireless networkswith a focus on propagation models," IEEE Transactions on Antennas and Propagation, vol. 65, no. 12, pp. 6213–6230, 2017.

[5] W. El-Halwagy, R. Mirzavand, J. Melzer, M. Hossain, and P. Mousavi, "Investigation of wideband substrate-integrated vertically-polarized electric dipole antenna and arrays for mm-wave 5G mobile devices," IEEE Access, vol. 6, pp. 2145–2157, 2017.

[6] Q. Cai, Y. Li, X. Zhang, and W. Shen, "Wideband MIMO antenna array covering 3.3-7.1 GHz for 5G metal-rimmed smartphone applications," IEEE Access, vol. 7, pp. 142070– 142084, 2019.

[7] Z. Ren and A. Zhao, "Dual-band MIMO antenna with compact self-decoupled antenna pairs for 5G mobile applications," IEEE Access, vol. 7, pp. 82288–82296, 2019.

[8] M. Abdullah, Y.-L. Ban, K. Kang, M.-Y. Li, and M. Amin, "Eight-element antenna array at 3.5 Ghz for mimo wireless application," Progress In Electromagnetics Research C, vol. 78, pp. 209–216, 2017.

[9] H. Al-Saif, M. Usman, M. T. Chughtai, and J. Nasir, "Compact ultra-wide band MIMO antenna system for lower 5G bands," Wireless Communications and Mobile Computing, vol. 2018, Article ID 2396873, 6 pages, 2018

[10] D. EL Hadri, A. Zugari, and A. Zakriti, "*e study of a 5G antenna with encoche and defected ground structure (DGS) using the

iterative method," in Proccedings of the IEEE, WITS, Fez, Morocco, April 2019.
[11] D. EL Hadri, A. Zugari, and A. Zakriti, "Analysis of a 38 GHz band Antenna for 5G wireless communication using wave concept iterative procedure (WCIP) method," in Proceedings of the EAI, ICCWCS, K´enitra, Morocco, April 2019.
[12] N. Ojaroudiparchin, M. Shen, and G. F. Pedersen, "A 28 GHz FR-4 compatible phased array antenna for 5G mobile phone applications," in Proceedings of the IEEE, ISAP, Hobart, TAS, Australia, December 2015.
[13] A. C. S. Jr, I. F. da Costa, R. A. dos Santos, H. R. D. Filgueiras, and D. H. Spadoti, "Waveguide-based antenna arrays for 5G networks," International Journal of Antennas and Propagation, 2018.
[14] M. C. Jose, S. Radha, B. S. Sreeja, and P. Kumar, "Design of 28 GHz high gain 5G MIMO antenna array system,," in Proceedings of the IEEE Region 10 Annual International Conference, TENCON, pp. 1913–1916, Kochi, India, October 2019.
[15] Y. Rahayu, I. P. Sari, D. I. Ramadhan, and R. Ngah, "High gain 5G MIMO antenna for mobile base station," International Journal of Electrical and Computer Engineering (IJECE), vol. 9, no. 1, pp. 468–476, 2019.
[16] M. Khalid, I. N. Syeda, H. Niamat et al., "4-port MIMO antenna with defected ground structure for 5G millimeter wave applications," Electronics, vol. 9, no. 1, 2020.
[17] H. M. Marzouk, M. I. Ahmed, and A.-E. H. Shaalan, "Novel dual-band 28/38 GHz MIMO antennas for 5g mobile applications," Progress In Electromagnetics Research C, vol. 93, pp. 103–117, 2019.
[18] Y. Zhang, J.-Y. Deng, M.-J. Li, D. Sun, and L.-X. Guo, "A MIMO dielectric resonator antenna with improved isolation for 5G mm-wave applications," IEEE Antennas and Wireless Propagation Letters, vol. 18, no. 4, pp. 747–751, 2019.
[19] Z. Wani, M. P. Abegaonkar, and S. K. Koul, "A 28-GHz antenna for 5G MIMO applications," Progress In Electromagnetics Research Letters, vol. 78, pp. 73–79, 2018.
[20] M. N. Hasan and M. Seo, "Compact omnidirectional 28 GHz 2×2 MIMO antenna array for 5G communications," in Proceedings of the International Symposium on Antennas and Propagation (ISAP), Busan, Korea, October 2018.
[21] M. S. Sharawi, S. K. Podilchak, M. T. Hussain, and Y. M. M. Antar, "Dielectric resonator-based MIMO antenna system enabling millimetre-wave mobile devices," IET Microwaves, Antennas & Propagation, vol. 11, no. 2, pp. 287–293, 2017.
[22] S. Gupta, Z. Briqech, A. R. Sebak, and T. Ahmed Denidni, "Mutual-coupling reduction using metasurface corrugations for 28 GHz MIMO applications," IEEE Antennas and Wireless Propagation Letters, vol. 16, pp. 2763–2766, 2017.
[23] N. K. Mallat, M. Ishtiaq, A. Ur Rehman, and A. Iqbal, "Millimeter-wave in the face of 5G communication potential applications," IETE Journal of Research, pp. 1–9, 2020.
[24] T. S. Rappaport, R. Shu Sun, R. Mayzus et al., "Millimeter wave mobile communications for 5G cellular: it will work!" IEEE Access, vol. 1, pp. 335–349, 2013.
[25] C. K. Agubor, I. Akwukwuegbu, M. Olubiwe et al., "A comprehensive review on the feasibility and challenges of millimeter wave in emerging 5G mobile communication," Advances in Science, Technology and Engineering Systems Journal, vol. 4, no. 3, pp. 138–144, 2019.
[26] M. Xiao, S. Mumtaz, Y. Huang et al., "Millimeter wave communications for future mobile networks," IEEE Journa+